arXiv:1701.04874v1 [cond-mat.supr-con] 17 Jan 2017

Phase diagram and neutron spin resonance of superconducting $NaFe_{1-x}Cu_xAs$

Guotai Tan,[1] Yu Song,[2,*] Rui Zhang,[2] Lifang Lin,[1] Zhuang Xu,[1] Long Tian,[1] Songxue Chi,[3] Barry Winn,[3] M. K. Graves-Brook,[3] Shiliang Li,[4,5] and Pengcheng Dai[2,1,†]

[1]*Department of Physics, Beijing Normal University, Beijing 100875, China*
[2]*Department of Physics and Astronomy, Rice University, Houston, Texas 77005, USA*
[3]*Quantum Condensed Matter Division, Oak Ridge National Laboratory, Oak Ridge, Tennessee 37831, USA*
[4]*Beijing National Laboratory for Condensed Matter Physics, Institute of Physics, Chinese Academy of Sciences, Beijing 100190, China*
[5]*Collaborative Innovation Center of Quantum Matter, Beijing 100190, China*

We use transport and neutron scattering to study the electronic phase diagram and spin excitations of $NaFe_{1-x}Cu_xAs$ single crystals. Similar to Co- and Ni-doped NaFeAs, a bulk superconducting phase appears near $x \approx 2\%$ with the suppression of stripe-type magnetic order in NaFeAs. Upon further increasing Cu concentration the system becomes insulating, culminating in an antiferromagnetically ordered insulating phase near $x \approx 50\%$. Using transport measurements, we demonstrate that the resistivity in $NaFe_{1-x}Cu_xAs$ exhibits non-Fermi-liquid behavior near $x \approx 1.8\%$. Our inelastic neutron scattering experiments reveal a single neutron spin resonance mode exhibiting weak dispersion along c-axis in $NaFe_{0.98}Cu_{0.02}As$. The resonance is high in energy relative to the superconducting transition temperature T_c but weak in intensity, likely resulting from impurity effects. These results are similar to other iron pnictides superconductors despite the superconducting phase in $NaFe_{1-x}Cu_xAs$ is continuously connected to an antiferromagnetically ordered insulating phase near $x \approx 50\%$ with significant electronic correlations. Therefore, electron correlations is an important ingredient of superconductivity in $NaFe_{1-x}Cu_xAs$ and other iron pnictides.

PACS numbers:

I. INTRODUCTION

Superconductivity in copper-oxides is obtained by electron- or hole-doping into their antiferromagnetically ordered insulating parent compounds with strong electron correlations[1,2]. Superconductivity in iron pnictides, on the other hand, is derived from parent compounds that are bad metals[3–5]. Despite the metallic ground state of the parent compounds, strong electronic correlations are suggested to be present in iron pnictides[6–8], especially in heavily hole-doped systems[9–11]. In addition to replacing A in AFe_2As_2 (A = Ca, Sr, Ba) with alkaline metals (K, Na, Rb, Cs)[4,5], hole-doping in iron pnictides can be achieved through Mn or Cr doping on Fe site although no superconductivity is induced in these cases[12,13]. Doping Cu on Fe site presents an intriguing case, whereas at low doping levels Cu is suggested to dope electrons[14], at higher concentrations Cu has a $3d^{10}$ configuration and acts as a hole-dopant[15,16]. However, in Cu doped AFe_2As_2, resistivity remains $\rho < 1\text{m}\Omega \cdot \text{cm}$ throughout the whole phase diagram with no signs of strengthened electronic correlations[16]. As the As atoms within the same unit cell of $AFe_{2-x}Cu_xAs_2$ can form $[As]^{-3} \equiv [As\text{-}As]^{-4}/2$ covalent bond with increasing Cu-doping and reducing As-As distance[15,16], large Cu-doping therefore has little effect on the valence of Fe and ACu_2As_2 becomes a *sp*-metal without electron correlations as predicted by band structure calculations[17].

Since the crystal structure of $NaFe_{1-x}Cu_xAs$ does not allow the formation of As-As covalent bond [Fig. 1(a)][18], heavily doped $NaFe_{1-x}Cu_xAs$ is a candidate system to tune the strength of electronic correlations[19]. Recent transport[18], scanning tunneling microscopy (STM)[20], angle-resolved photoemission spectroscopy[21], and optical conductivity[22] measurements demonstrated that with significant ($> 10\%$) Cu doping, $NaFe_{1-x}Cu_xAs$ acquires an insulating ground state. Diffraction measurements revealed short-range Fe-Cu cation order and magnetic order develops as the system becomes insulating. With increasing x, the Fe-Cu cation order and magnetic order continuously increase in correlation lengths, and become long-range when $x \approx 50\%$[19]. The antiferromagnetically ordered insulating state in $NaFe_{1-x}Cu_xAs$ is a result of significant electronic correlations[19]. Compared to Cu-doped AFe_2As_2, $NaFe_{1-x}Cu_xAs$ is more correlated because of its larger iron pnictogen height which results in a small magnetic excitation bandwidth[23,24], hole-doping effect of Cu in $NaFe_{1-x}Cu_xAs$ is not counteracted by the formation of As-As covalent bonds and the local potential differences between Cu and Fe reduces the hopping between Fe sites[19]. Since the antiferromagnetically ordered Mott insulating phase of $NaFe_{1-x}Cu_xAs$ at $x \approx 0.5$ is continuously connected to an albeit somewhat far away superconducting phase at $x \approx 0.02$[18,19], it would be important to elucidate whether the superconducting state in $NaFe_{1-x}Cu_xAs$[18] is similar to other iron pnictide systems.

One hallmark of unconventional superconductivity in iron pnictides is the appearance of a neutron spin resonance mode in the superconducting state at the antiferromagnetic (AF) ordering wave vector of their parent compounds[5,25–27]. The energy of the resonance approximately scales with the superconducting transition temperature T_c or the superconducting gap Δ[27,28]. The

appearance of the resonance mode is typically accompanied by gapping of the normal state spectral weight below the resonance energy[5,25–27]. Both the resonance and the associated spin gap are typically interpreted as due to quasi-nested Fermi surfaces that results in a collective bound-state inside the superconducting gap[26,29,30]. Within this picture, the resonance mode is evidence for unconventional superconductivity with sign-changing superconducting order parameters on different parts of the Fermi surface[25]. The resonance in $BaFe_2As_2$-derived superconductors display significant dispersion along c-axis in the underdoped regime[31], and becomes L-independent in the well-overdoped region[32]. In electron-doped $NaFe_{1-x}Co_xAs$, two resonance modes are seen in underdoped compositions[24], with the lower-energy-mode gradually losing spectral weight upon further doping before disappearing near optimal doping[33,34]. The energy of the single resonance mode in well-overdoped $NaFe_{1-x}Co_xAs$ does not scale with T_c, likely due to multi-orbital physics and impurity effects[33]. Since superconducting domes are absent in Cu-doped AFe_2As_2[16,35], it is unclear if superconductivity induced by Cu-doping has similar electronic and magnetic properties as their electron/hole-doped counterparts. As $NaFe_{1-x}Cu_xAs$ exhibits bulk superconductivity similar to those of $NaFe_{1-x}Co_xAs$[18], superconducting $NaFe_{1-x}Cu_xAs$ offers a unique case to study the effect of the stronger impurity potential of Cu[18,36] on the resonance mode.

In this work, we use transport and magnetic susceptibility measurements to characterize $NaFe_{1-x}Cu_xAs$ with $x \leq 0.06$ and inelastic neutron scattering to study the neutron spin resonance in slightly overdoped $NaFe_{0.98}Cu_{0.02}As$. The temperature dependence of resistivity display an evolution from Fermi liquid behavior in NaFeAs, to non-Fermi-liquid behavior near $x = 0.018$ and back to Fermi-liquid behavior near $x = 0.032$, pointing to a funnel of quantum critical behavior near optimal doping. A single resonance mode that disperses weakly along c-axis is seen in $NaFe_{0.98}Cu_{0.02}As$, similar to slightly overdoped $NaFe_{1-x}Co_xAs$[34]. Similar to what was found in heavily overdoped $NaFe_{1-x}Co_xAs$[33], the resonance mode is at an higher energy than what is expected from scaling with T_c, likely related to the stronger impurity potential of Cu compared to Co[18,36], despite the low Cu concentration of 2%. The presence of both a putative quantum critical point in the phase diagram and a neutron spin resonance in superconducting $NaFe_{1-x}Cu_xAs$ is similar to other iron pnictide superconductors. Since $NaFe_{1-x}Cu_xAs$ can be continuously tuned to an antiferromagnetically ordered insulating phase with significant electronic correlations near $x \approx 0.5$[19], these results suggest electronic correlations to be an essential ingredient of superconductivity in iron pnictides.

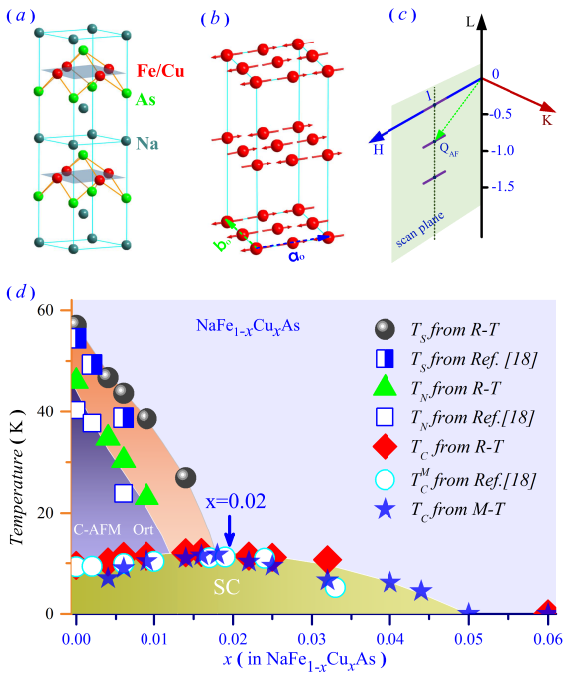

FIG. 1: (Color online) (a) Crystal structure of NaFeAs, two tetragonal unit cells stacked along the c-axis are shown. The orthorhombic unit cell is twice the size of the tetragonal unit cell with $a_O \approx \sqrt{2}a_T$ and $b_O \approx \sqrt{2}b_T$ and rotated by 45° compared to the tetragonal unit cell. (b) The magnetic structure of NaFeAs, only Fe atoms are shown. The magnetic unit cell is twice the size of the orthorhombic unit cell along c-axis. (c) Schematic of $[H, 0, L]$ scattering plane. (d) Phase diagram of $NaFe_{1-x}Cu_xAs$ obtained from magnetic susceptibility and resistivity measurements, results from previous work[18] are shown for comparison. The vertical arrow marks $x = 0.02$, for which inelastic neutron scattering measurements were carried out.

II. EXPERIMENTAL RESULTS

Single crystals of $NaFe_{1-x}Cu_xAs$ were prepared using the self-flux method method as described in previous work[37]. Inductively coupled plasma atomic emission spectroscopy previously revealed the actual Cu concentration to be similar to the nominal one for $x \lesssim 20\%$[19], we therefore quote nominal concentrations throughout this work, which is also consistent with previous report on $NaFe_{1-x}Cu_xAs$ in the superconducting region[18]. Resistivity and magnetic susceptibility measurements were carried out using commercial systems from Quantum Design. Resistivity is measured with the four-probe method, and magnetic susceptibility is measured upon warming with an in-plane magnetic field of 20 Oe after zero-field-cooling. Inelastic neutron scattering experiments were carried out using the HB-3 triple-axis spectrometer at the High Flux Isotope Reactor (HFIR) and the Hybrid Spectrometer (HYSPEC) at the Spallation

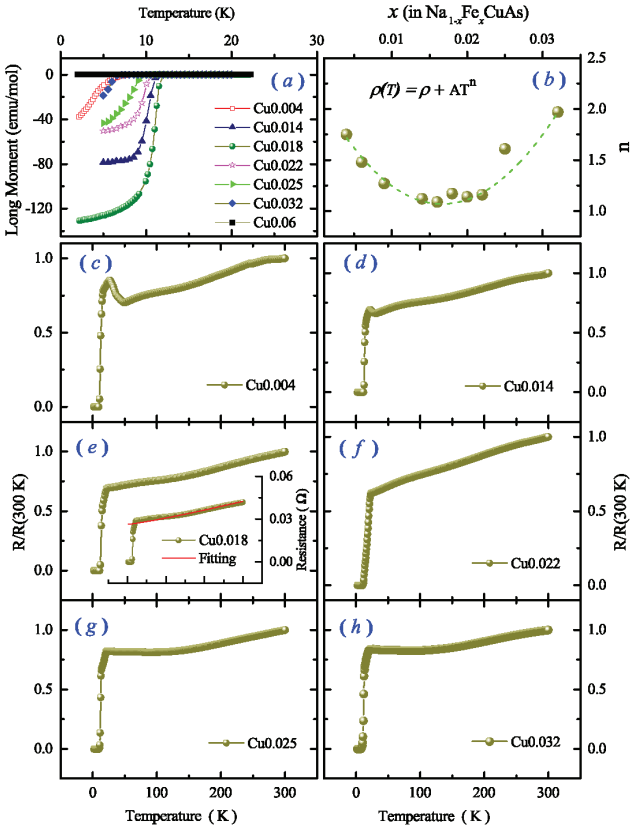

FIG. 2: (Color online) (a) Magnetic susceptibility of $NaFe_{1-x}Cu_xAs$ measured upon warming after zero-field-cooling. (b) n extracted from fitting resistivity of $NaFe_{1-x}Cu_xAs$ to the form $\rho = \rho_0 + AT^n$, the solid line is a guide-to-the-eye. (c)-(h) respectively shows resistivity of $NaFe_{1-x}Cu_xAs$ with $x = 0.004$, 0.014, 0.018, 0.022, 0.025 and 0.032 normalized to room temperature resistivity. The inset in (e) shows raw data for $x = 0.018$ and a typical fit to the empirical form mentioned in the text.

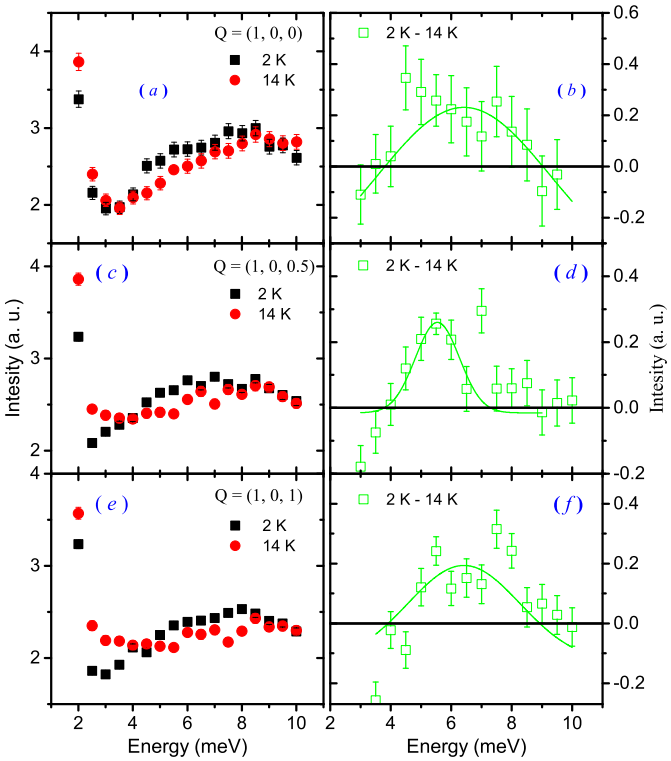

FIG. 3: (Color online) Constant-$\mathbf{Q}$ scans at $\mathbf{Q} = (1, 0, L)$ for (a) $L = 0$, (c) $L = 0.5$ and (e) $L = 1$. The difference of magnetic intensity in the superconducting state and the normal state for (b) $L = 0$, (d) $L = 0.5$ and (f) $L = 1$. The solid lines are fits to Gaussian peaks, which provide a rough estimate of the peak center of the resonance mode. The fits in (b) and (f) are constrained to have the same center.

Neutron Source, both at Oak Ridge National Laboratory. The experiment at HB-3 used a pyrolitic graphite monochromtor, analyzer and filter after the sample, the collimation used is 48′-40′ -sample-40′-120′ and the final neutron energy is fixed to $E_f = 14.7$ meV. HYSPEC is a time-of-flight chopper spectrometer with a movable strip-shaped detector bank that has much fewer pixels along the vertical direction compared to the horizontal direction. Detected neutron counts from the middle third of the pixels along the vertical direction are binned making it function like a triple-axis spectrometer with a position-sensitive-detector, and by rotating the sample and the detector bank, maps of the scattering plane can be obtained. Fixed incident energy $E_i = 15$ meV is used for the experiment on HYSPEC. Momentum transfer $\mathbf{Q} = (Q_x, Q_y, Q_z)$ is presented in reciprocal lattice units (r.l.u.) as (H, K, L), with $H = Q_x a/2\pi$, $K = Q_y b/2\pi$ and $L = Q_z c/2\pi$. We adopt the chemical unit cell for the orthorhombic phase of $NaFe_{1-x}Cu_xAs$, in this notation $a \approx b \approx 5.56$ and $c \approx 7.05$ for NaFeAs[38]. The orthorhombic unit cell is twice the volume of the tetragonal unit cell [Fig. 1(a)], in this notation magnetic Bragg peaks are seen at $\mathbf{Q} = (1, 0, L)$ with $L = 0.5, 1.5, 2.5\ldots$, corresponding to half of the magnetic unit cell along c-axis [Fig. 1(b)]. 8 high-quality single crystals with a total mass of 6.04 grams were co-aligned in the $[H, 0, L]$ scattering plane [Fig. 1(c)].

Figure 2 summarizes magnetic susceptibility and resistivity measurements. As can be seen in Fig. 2(a) optimal superconductivity with $T_c \approx 11.8$ K is obtained near $x = 0.018$ in agreement with previous results[18]. Normalized resistivity in $NaFe_{1-x}Cu_xAs$ with $x = 0.004$, 0.014, 0.018, 0.022, 0.025 and 0.032 are shown in Fig. 2(c) through Fig. 2(h). For underdoped samples ($x = 0.004$ and 0.014), resistivity exhibits clear kinks at T_s and T_N before vanishing in the superconducting state below T_c. Resistivity data in the tetragonal paramagnetic metallic state are fit to the empirical form $\rho = \rho_0 + AT^n$ for all measured samples [inset of Fig. 2(e)], similar to previous work on $NaFe_{1-x}Co_xAs$[39,40]. A Fermi-liquid corresponds to $n = 2$, whereas linear resistivity ($n = 1$) is often ob-

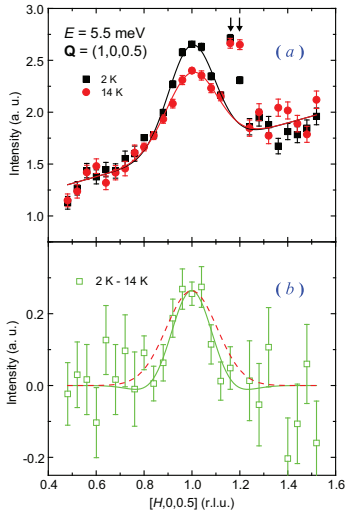

FIG. 4: (Color online) (a) H-scans at $E = 5.5$ meV centered at $\mathbf{Q} = (1, 0, 0.5)$. Solid lines are fits to Gaussian peaks with the linear background restrained to be the same for 2 K and 14 K. The two positions marked by arrows are contaminated by spurious scattering and are not used in the fits. (b) The difference between 2 K and 14 scans in (a), the solid line is the difference between the fits at 2 K and 14 K. The red dashed line is a Gaussian peak with width of the data at 14 K, shown for comparison. Fitting the difference to a Gaussian peak [not shown] results in a much narrower peak [FWHM = 0.17(3) (r.l.u.)] compared to the 14 K data [FWHM = 0.25(1) (r.l.u.)].

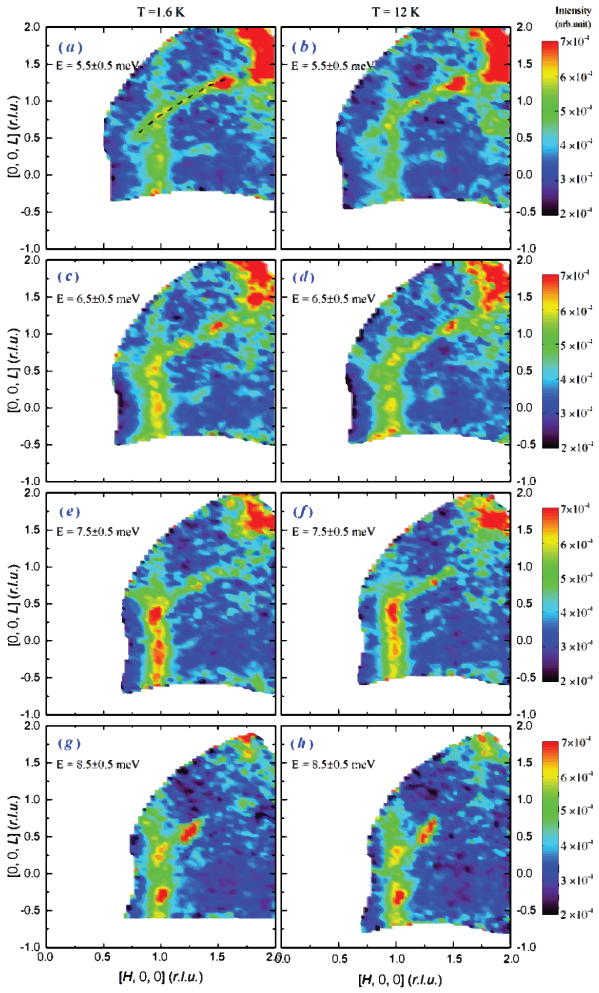
T = 1.6 K
T = 12 K
Intensity (arb.unit)
(a) E = 5.5±0.5 meV
(b) E = 5.5±0.5 meV
(c) E = 6.5±0.5 meV
(d) E = 6.5±0.5 meV
(e) E = 7.5±0.5 meV
(f) E = 7.5±0.5 meV
(g) E = 8.5±0.5 meV
(h) E = 8.5±0.5 meV
[0, 0, L] (r.l.u.)
[H, 0, 0] (r.l.u.)

FIG. 5: (Color online) Constant-energy maps in $[H, 0, L]$ scattering plane at $T = 1.6$ K for (a) $E = 5.5 \pm 0.5$ meV, (c) $E = 6.5 \pm 0.5$ meV, (e) $E = 7.5 \pm 0.5$ meV and (g) $E = 8.5 \pm 0.5$ meV. The corresponding results at $T = 12$ K are shown in panels (b), (d), (f) and (h). The streak of signal marked by the dashed line in (a) is spurious, as are similar signals in other panels.

served near a quantum critical point[41,42]. Doping dependence of n for $NaFe_{1-x}Cu_xAs$ is summarized in Fig. 2(b), revealing clear evolution from $n \approx 2$ in NaFeAs to $n \approx 1$ for $x = 0.018$, and back to $n \approx 2$ for $x = 0.032$. Similar behavior has been observed in other iron pnictide systems[39–43]. Based on magnetic susceptibility and resistivity measurements, we construct the phase diagram of $NaFe_{1-x}Cu_xAs$ near the superconducting dome as shown in Fig. 1(d), the obtained phase diagram is consistent with previous results[18].

Constant-$\mathbf{Q}$ scans at $\mathbf{Q} = (1, 0, L)$ for slightly overdoped $NaFe_{0.98}Cu_{0.02}As$ ($T_c = 11.8$ K and no static magnetic signal is observed) measured using HB-3 are summarized in Figure 3. Scans above ($T = 14$ K) and below ($T = 2$ K) T_c for $L = 0$, 0.5 and 1 are shown in Fig. 3(a), (c) and (e), respectively. The corresponding 2 K data after subtracting 14 K data are similarly shown in Fig. 3(b), (d) and (f). A clear resonance mode that displays a weak c-axis dispersion accompanied by a spin gap at lower energies can be clearly seen. For $L = 0.5$ [Fig. 3(d)], corresponding to the magnetic zone center in magnetically ordered NaFeAs, the resonance is centered at around $E \approx 5.5$ meV. Similarly for $L = 0$ and 1 [Fig. 3(b), (f)], corresponding to the magnetic zone boundary along c-axis in magnetically ordered NaFeAs, the resonance is centered at $E \approx 6.5$ meV. The resonance mode at $L = 0.5$ also appears to be sharper than for $L = 0$ and 1, this behavior is different from slightly overdoped $NaFe_{0.955}Co_{0.045}As$ in which width of the resonance mode does not depend on L[34].

H-scans at the peak of the resonance mode for $L = 0.5$ ($E = 5.5$ meV) is shown in Fig. 4. At both 2 K and 14 K, a clear peak is observed, with the peak at 2 K only slightly stronger than the one at 14 K [$\approx 23\%$ stronger from area of fits in Fig. 4(a)], meaning the resonance is weak compared to the normal state excitations in contrast to slightly overdoped $NaFe_{1-x}Co_xAs$[34] in which the resonance mode dominates the magnetic excitations in the superconducting state. Given the normal state spin fluctuations have indistinguishable intensities in Co- and Cu-doped $BaFe_2As_2$[36], it is reason-

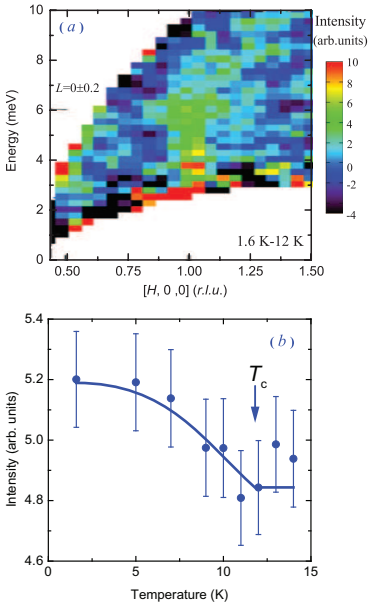

FIG. 6: (Color online) (a) H-energy map of 1.6 K data subtract by 12 K data obtained by binning data with $-0.2 \leq L \leq 0.2$. (b) Temperature dependence of the resonance mode, obtained by binning data with $4.5 \leq E \leq 6.5$ meV, $0.87 \leq H \leq 1.13$ and $-0.2 \leq L \leq 0.2$. The arrow marks T_c, and the solid line is a guide-to-the-eye.

able to assume the normal state intensities in Co- and Cu-doped NaFeAs are also similar. Therefore, compared to $NaFe_{0.955}Co_{0.045}As$[34], the resonance mode in $NaFe_{0.98}Cu_{0.02}As$ is also quantitatively much weaker. The width of the magnetic peak for $E = 5.5$ meV at 2 K [FWHM = 0.228(8) (r.l.u.)] and 14 K [FWHM = 0.25(1) (r.l.u.)] are similar with the peak in the superconducting state slightly narrower, similar to slightly overdoped $NaFe_{1-x}Co_xAs$[34]. The change in peak width can be seen more clearly by examining the difference of 2 K and 14 K data [Fig. 4(b)], which is significantly narrower than the 14 K data itself [Gaussian peak in red dashed line], with FWHM = 0.17(3) (r.l.u.). This suggests that the effect of superconductivity is not only to enhance intensity at the energy of the resonance mode, but also to increase the correlation length of magnetic excitations. The resonance being more well-defined in momentum space compared the normal state excitations can result from reduction of damping due to opening of the superconducting gap, or the resonance mode intrinsically having a longer correlation length. A weak neutron spin resonance mode is seen in $Ba(Fe_{1-x}Ru_x)_2As_2$ near optimal doping and ascribed to weakened electronic correlations[44]. In comparison, the weak resonance in $NaFe_{0.98}Cu_{0.02}As$ is likely due to impurity effects given electronic correlations in superconducting $NaFe_{1-x}Co_xAs$ and $NaFe_{1-x}Cu_xAs$ should be similar.

Our results are further substantiated by data obtained using HYSPEC in Figure 5 and 6. Constant-energy maps of the $[H, 0, L]$ scattering plane are shown in Figure 5 at $T = 1.6$ K and 12 K, as can be clearly seen magnetic excitations form rods centered at $H = 1$ with little L-dependence in both the normal and the superconducting state. In magnetically ordered NaFeAs, c-axis polarized spin waves exhibit a spin gap of $E_g \approx 4.5$ meV at $\mathbf{Q} = (1, 0, 0.5)$ and $E_g \approx 7$ meV at $\mathbf{Q} = (1, 0, 1)$[45]. Upon Co-doping into the slightly overdoped regime, magnetic excitations become L-independent[34]. Therefore, the reduction of effective c-axis magnetic coupling by doping Cu doping into NaFeAs is similar to doping Co, such behavior is also seen in Ni-doped $BaFe_2As_2$[46]. By comparing the Fig. 5(a) and (b) or Fig. 5(c) and (d), which are plotted to the same color scale, it is clear that the intensities differ little in the superconducting and normal state, consistent with resonance mode being weak. In addition to the magnetic signal, we also observe streaks of spurious scattering of unknown origin [dashed line in Fig. 5(a)]. While the spurious signal overlaps with the magnetic signal at $L = 0.5$, the magnetic signal at $L = 0$ is reasonably far away. In Fig. 6(a) we show the 1.6 K data subtracted by 12 K data by binning points with $L = 0 \pm 0.2$, which avoids potential contamination from the spurious signal. Similar to Fig. 3(b) and (f), a resonance that is rather broad in energy is seen. The temperature dependence of the resonance mode at $L = 0$ is shown in Fig. 6(b), an superconducting-order-parameter-like increase below T_c is observed.

III. DISCUSSION AND CONCLUSION

The weak resonance mode in $NaFe_{1-x}Cu_xAs$ is likely a result of the stronger impurity potential of Cu, which is also likely responsible for the lower optimal T_c in $NaFe_{1-x}Cu_xAs$[18] compared to $NaFe_{1-x}Co_xAs$[39,40] and the near-absence of superconductivity in $Ba(Fe_{1-x}Cu_x)_2As_2$[35]. Compared to $Ba(Fe_{1-x}Cu_x)_2As_2$ in which superconductivity is nearly absent, the presence of a superconducting dome in $NaFe_{1-x}Cu_xAs$ may be related to the lower Cu concentration needed to suppress the magnetic order. In a similar vein, lower concentration of Ni in $NaFe_{1-x}Ni_xAs$ was found to cause magnetic order to remain long-range and commensurate approaching optimal superconductivity[47], in contrast to Co- and Ni-doped $BaFe_2As_2$ in which the magnetic order becomes short-range and incommensurate near optimal-doping[48,49]. The impurity potential and concentration of dopants therefore has significant effects on the physical properties of iron pnictide superconductors.

The resonance mode in slightly overdoped $NaFe_{0.98}Cu_{0.02}As$ with $T_c = 11.8$ K is at $E \approx 5.5$ meV for $L = 0.5$, corresponding to $E_r \approx 5.5 k_B T_c$. This is higher than $E_r \approx 4.3 k_B T_c$ suggested for doped $BaFe_2As_2$[27] and $E_r \approx 4.5 k_B T_c$ in slightly overdoped $NaFe_{0.955}Co_{0.045}As$[34] but lower than $E_r \approx 7.1 k_B T_c$ in heavily overdoped $NaFe_{0.92}Co_{0.08}As$[33]. Therefore, due to multi-orbital physics and impurity effects, there

appears to be no simple relationship between E_r and T_c in doped NaFeAs. Specifically, both the concentration of dopants [slightly overdoped and heavily overdoped $NaFe_{1-x}Co_xAs$] and impurity potential of dopants [slightly overdoped $NaFe_{1-x}Co_xAs$ and $NaFe_{1-x}Cu_xAs$] seem to increase the ratio E_r/k_BT_c. In cuprate superconductors it was found spectral weight of the resonance mode scales linearly with $(E_c - E_r)/E_c$[50], where E_c is threshold of the particle-hole continuum. This means as E_r moves closer to the particle-hole continuum, spectral weight of the resonance also collapses. A similar effect might also contribute to the weak resonance mode in $NaFe_{0.98}Cu_{0.02}As$, as the high ratio of E_r and k_BT_c suggests the resonance is likely closer to the particle-hole continuum compared to $NaFe_{0.955}Co_{0.045}As$.

Similarly, the broader resonance at $L = 0$ and 1 compared to $L = 0.5$ in $NaFe_{0.98}Cu_{0.02}As$ [Fig. 3(b), (d) and (f)] may be due to the mode at $L = 0$ and 1 being at a higher energy, and experience stronger interactions with particle-hole excitations that broaden the mode. Alternatively, spin-orbit coupling found to be present in many iron pnictide superconductors[51] and causes energy-splitting of resonance modes polarized along different crystallographic directions[52,53], also results in broadening of the resonance mode seen in unpolarized neutron scattering experiments. Polarized neutron scattering experiments are needed to distinguish between these scenarios.

The superconducting phase in $NaFe_{1-x}Cu_xAs$ near $x \approx 0.02$ can be continuously tuned to the antiferromagnetically ordered insulating phase with significant electronic correlations near $x \approx 0.5$ through a region of short-range cation and magnetic order[19], pointing to the possibility of the generic phase diagram of iron pnictides to be anchored around a Mott-insulating state[10,20]. The observation of a spin resonance mode in superconducting $NaFe_{1-x}Cu_xAs$ demonstrates that the superconducting state is similar to other iron pnictide superconductors, and therefore electronic correlations should be an integral part of the physics of iron pnictide superconductors.

IV. ACKNOWLEDGMENTS

The single crystal growth and neutron scattering work at Rice is supported by the U.S. DOE, BES under contract no. de-sc0012311 (P.D.). A part of the material synthesis work at Rice is supported by the Robert A. Welch Foundation Grant No. C-1839 (P.D.). Research at BNU and IOP are supported by the National Basic Research Program of China (973 Program, Grants No. 2012CB821401), National Natural Science Foundation of China (Grants No. 11374011), and the Fundamental Research Funds for the Central Universities (Grants No. 2014KJJCB27). Research at Oak Ridge National Laboratory's HFIR was sponsored by the Scientific User Facilities Division, Office of Basic Energy Sciences, U.S. Department of Energy.

* Electronic address: Yu.Song@rice.edu
† Electronic address: pdai@rice.edu

[1] P. A. Lee, N. Nagaosa, and X.-G. Wen, Rev. Mod. Phys. **78**, 17 (2006).
[2] B. Keimer, S. A. Kivelson, M. R. Norman, S. Uchida, and J. Zaanen, Nature (London) **518**, 179 (2015).
[3] Y. Kamihara, T. Watanabe, M. Hirano. and H. Hosono, J. Am. Chem. Soc. **130**, 3296-3297 (2008).
[4] G. R. Stewart, Rev. Mod. Phys. **83**, 1589-1652 (2011).
[5] P. C. Dai, Rev. Mod. Phys. **87**, 855(2015).
[6] Q. Si, and E. Abrahams, Phys. Rev. Lett. **101**, 076401 (2008).
[7] H. Ishida, and A. Liebsch, Phys. Rev. B **81**, 054513 (2010).
[8] T. Misawa, K. Nakamura, and M. Imada, Phys. Rev. Lett. **108** 177007 (2012).
[9] F. Hardy, A. E. Böhmer, D. Aoki, P. Burger, T. Wolf, P. Schweiss, R. Heid, P. Adelmann, Y. X. Yao, G. Kotliar, J. Schmalian, and C. Meingast, Phys. Rev. Lett. **111**, 027002 (2013).
[10] L. de' Medici, G. Giovannetti, and M. Capone, Phys. Rev. Lett. **112** 177001 (2014).
[11] M. Nakajima *et al.*, J. Phys. Soc. Jpn. **83**, 104703 (2014).
[12] A. Thaler, H. Hodovanets, M. S. Torikachvili, S. Ran, A. Kracher, W. Straszheim, J. Q. Yan, E. Mun, and P. C. Canfield, Phys. Rev. B **84**, 144528 (2011).
[13] Athena S. Sefat, David J. Singh, Lindsay H. VanBebber, Yurij Mozharivskyj, Michael A. McGuire, Rongying Jin, Brian C. Sales, Veerle Keppens, and David Mandrus, Phys. Rev. B **79**, 224524 (2009).
[14] S. Ideta, T. Yoshida, I. Nishi, A. Fujimori, Y. Kotani, K. Ono, Y. Nakashima, S. Yamaichi, T. Sasagawa, M. Nakajima, K. Kihou, Y. Tomioka, C. H. Lee, A. Iyo, H. Eisaki, T. Ito, S. Uchida, and R. Arita, Phys. Rev. Lett. **110**, 107007 (2013).
[15] V. K. Anand, P. K. Perera, Abhishek Pandey, R. J. Goetsch, A. Kreyssig, and D. C. Johnston, Phys. Rev. B **85** 214523 (2012).
[16] Y. J. Yan, P. Cheng, J. J. Ying, X. G. Luo, F. Chen, H. Y. Zou, A. F. Wang, G. J. Ye, Z. J. Xiang, J. Q. Ma, and X. H. Chen, Phys. Rev. B **87**, 075105 (2013).
[17] D. J. Singh, Phys. Rev. B **79**, 153102 (2009).
[18] A. F. Wang, J. J. Lin, P. Cheng, G. J. Ye, F. Chen, J. Q. Ma, X. F. Lu, B. Lei, X. G. Luo, and X. H. Chen, Phys. Rev. B **88**, 094516 (2013).
[19] Yu Song, Zahra Yamani, Chongde Cao, Yu Li , Chenglin Zhang, Justin S. Chen, Qingzhen Huang, Hui Wu, Jing Tao, Yimei Zhu, Wei Tian, Songxue Chi, Huibo Cao, Yao-Bo Huang, Marcus Dantz, Thorsten Schmitt, Rong Yu, Andriy H. Nevidomskyy, Emilia Morosan, Qimiao Si, and Pengcheng Dai, Nat. Commun. **7**, 13879 (2016).
[20] Cun Ye, Wei Ruan, Peng Cai, Xintong Li, Aifeng Wang, Xianhui Chen, and Yayu Wang, Phys. Rev. X **5**, 021013 (2015).
[21] C.E. Matt, N. Xu, Baiqing Lv, Junzhang Ma, F. Bisti,

J. Park, T. Shang, Chongde Cao, Yu Song, Andriy H. Nevidomskyy, Pengcheng Dai, L. Patthey, N.C. Plumb, M. Radovic, J. Mesot, and M. Shi, Phys. Rev. Lett. **117**, 097001 (2016).

[22] A. Charnukha *et al.*, unpublished work.

[23] Z. P. Yin, K. Haule, and G. Kotliar, Nat. Mater. **10**, 932 (2011).

[24] Chenglin Zhang, Rong Yu, Yixi Su, Yu Song, Miaoyin Wang, Guotai Tan, Takeshi Egami, J. A. Fernandez-Baca, Enrico Faulhaber, Qimiao Si, and Pengcheng Dai, Phys. Rev. Lett. **111**, 207002 (2013).

[25] A. D. Christianson, E. A. Goremychkin, R. Osborn, S. Rosenkranz, M. D. Lumsden, C. D. Malliakas, I. S. Todorov, H. Claus, D. Y. Chung, M. G. Kanatzidis, R. I. Bewley, and T. Guidi, Nature **456**, 930 (2008).

[26] D. J. Scalapino, Rev. Mod. Phys. **84**, 1383 (2012).

[27] D. S. Inosov, J. T. Park, A. Charnukha, Yuan Li, A. V. Boris, B. Keimer, and V. Hinkov, Phys. Rev. B 83, 214520 (2011).

[28] G. Yu, Y. Li, E. M. Motoyama, and M. Greven, Nat. Phys. **5**, 873 (2009).

[29] M. Eschrig, Adv. Phys. **55**, 47-183 (2006).

[30] P. J. Hirschfeld, M. M. Korshunov, and I. I. Mazin, Rep. Prog. Phys. **74**, 124508 (2011).

[31] S. Chi, A. Schneidewind, J. Zhao, L. W. Harriger, L. Li, Y. Luo, G. Cao, Z. Xu,M. Loewenhaupt, J. Hu, and P. Dai, Phys. Rev. Lett. **102**, 107006 (2009).

[32] C. H. Lee, P. Steffens, N. Qureshi, M. Nakajima, K. Kihou, A. Iyo, H. Eisaki, M. Braden, Phys. Rev. Lett. **111**, 167002 (2013).

[33] Chenglin Zhang, Weicheng Lv, Guotai Tan, Yu Song, Scott V. Carr, Songxue Chi, M. Matsuda, A. D. Christianson, J. A. Fernandez-Baca, L. W. Harriger, and Pengcheng Dai, Phys. Rev. B **93**, 174522 (2016).

[34] Chenglin Zhang, H.-F. Li, Yu Song, Yixi Su, Guotai Tan, Tucker Netherton, Caleb Redding, Scott V. Carr, Oleg Sobolev, Astrid Schneidewind, Enrico Faulhaber, L. W. Harriger, Shiliang Li, Xingye Lu, Dao-Xin Yao, Tanmoy Das, A. V. Balatsky, Th. Brückel, J. W. Lynn, and Pengcheng Dai, Phys. Rev. B **88**, 064504 (2013).

[35] N. Ni, A. Thaler, J. Q. Yan, A. Kracher, E. Colombier, S. L. Bud'ko, P. C. Canfield, and S. T. Hannahs, Phys. Rev. B **82**, 024519 (2010).

[36] M. G. Kim, J. Lamsal, T. W. Heitmann, G. S. Tucker, D. K. Pratt, S. N. Khan, Y. B. Lee, A. Alam, A. Thaler, N. Ni, S. Ran, S. L. Budko, K. J. Marty, M. D. Lumsden, P. C. Canfield, B. N. Harmon, D. D. Johnson, A. Kreyssig, R. J. McQueeney, and A. I. Goldman, Phys. Rev. Lett. **109**, 167003 (2012).

[37] N. Spyrison, M. A. Tanatar, Kyuil Cho, Y. Song, P. C. Dai, C. L. Zhang, and R. Prozorov Phys. Rev. B **86**, 144528 (2012).

[38] Shiliang Li, Clarina de la Cruz, Q. Huang, G. F. Chen, T.-L. Xia, J. L. Luo, N. L. Wang, and Pengcheng Dai, Phys. Rev. B **80** 020504(R) (2009).

[39] Guotai Tan, Yu Song, Chenglin Zhang, Lifang Lin, Zhuang Xu, Tingting Hou, Wei Tian, Huibo Cao, Shiliang Li, Shiping Feng, and Pengcheng Dai, Phys. Rev. B **94**, 014509 (2016).

[40] A F Wang, J J Ying, X G Luo, Y J Yan, D Y Liu, Z J Xiang, P Cheng, G J Ye, L J Zou, Z Sun, and X. H. Chen, New J. Phys. **15**, 043048 (2013).

[41] S. Kasahara, T. Shibauchi, K. Hashimoto, K. Ikada, S. Tonegawa, R. Okazaki, H. Shishido, H. Ikeda, H. Takeya, K. Hirata, T. Terashima, and Y. Matsuda, Phys. Rev. B **81**, 184519 (2010).

[42] James G. Analytis, H-H. Kuo, Ross D. McDonald, Mark Wartenbe, P. M. C. Rourke, N. E. Hussey, and I. R. Fisher, Nat. Phys. **10**, 194 (2014).

[43] Huiqian Luo, Rui Zhang, Mark Laver, Zahra Yamani, Meng Wang, Xingye Lu, Miaoyin Wang, Yanchao Chen, Shiliang Li, Sung Chang, Jeffrey W. Lynn, and Pengcheng Dai, Phys. Rev. Lett. **108**, 247002 (2012).

[44] Jun Zhao, C. R. Rotundu, K. Marty, M. Matsuda, Y. Zhao, C. Setty, E. Bourret-Courchesne, Jiangping Hu, and R. J. Birgeneau, Phys. Rev. Lett. **110**, 147003 (2013).

[45] Yu Song, Louis-Pierre Regnault, Chenglin Zhang, Guotai Tan, Scott V. Carr, Songxue Chi, A. D. Christianson, Tao Xiang, and Pengcheng Dai, Phys. Rev. B **88**, 134512 (2013).

[46] Leland W. Harriger, Astrid Schneidewind, Shiliang Li, Jun Zhao, Zhengcai Li, Wei Lu, Xiaoli Dong, Fang Zhou, Zhongxian Zhao, Jiangping Hu, and Pengcheng Dai, Phys. Rev. Lett. **103**, 087005 (2009).

[47] Weiyi Wang *et al.*, unpublished neutron diffraction results (2016).

[48] D. K. Pratt, M. G. Kim, A. Kreyssig, Y. B. Lee, G. S. Tucker, A. Thaler, W. Tian, J. L. Zarestky, S. L. Bud'ko, P. C. Canfield, B. N. Harmon, A. I. Goldman, and R. J. McQueeney, Phys. Rev. Lett. **106**, 257001 (2011).

[49] Huiqian Luo, Rui Zhang, Mark Laver, Zahra Yamani, Meng Wang, Xingye Lu, Miaoyin Wang, Yanchao Chen, Shiliang Li, Sung Chang, Jeffrey W. Lynn, and Pengcheng Dai, Phys. Rev. Lett. **108**, 247002 (2012).

[50] M.K. Chan, Y. Tang, C.J. Dorow, J. Jeong, L. Mangin-Thro, M.J. Veit, Y. Ge, D.L. Abernathy, Y. Sidis, P. Bourges, and M. Greven, Phys. Rev. Lett. **117**, 277002 (2016).

[51] S. V. Borisenko, D. V. Evtushinsky, Z.-H. Liu, I. Morozov, R. Kappenberger, S. Wurmehl, B. Bchner, A. N. Yaresko, T. K. Kim, M. Hoesch, T. Wolf, and N. D. Zhigadlo, Nat. Phys. **12**, 311 (2016).

[52] M. M. Korshunov, Y. N. Togushova, I. Eremin, and P. J. Hirschfeld, J. Supercond. Novel Magn. **26**, 2873 (2013).

[53] Yu Song, Haoran Man, Rui Zhang, Xingye Lu, Chenglin Zhang, Meng Wang, Guotai Tan, L.-P. Regnault, Yixi Su, Jian Kang, Rafael M. Fernandes, and Pengcheng Dai, Phys. Rev. B **94**, 214516 (2016).